institutions performed ILBT, only 14% of all patients received ILBT combined with EBRT, indicating that this treatment modality was used only in selected cases because the effect of ILBT is limited to the area surrounding the lumen of the biliary tract and improvement in local control can therefore be expected only for small tumors [9].

The optimal radiation field for BTC remains to be defined. The majority of relapses after resection with curative intent occur at the primary tumor site [13], which suggests that it may be reasonable to limit RT to the primary tumor (bed). Only 23% of the patients included in this survey received radiation to the tumor (bed) as well as the regional lymph nodes, regardless of the lymph node status. Although limiting the radiation field to the tumor (bed) has tended to become prevalent in Japan, the definition of clinical target volume included regional lymph nodes as well as the tumor (bed) in a recent meta-analysis of 14 selected papers with detailed information on adjuvant RT after surgery [3], as well as in many reports on unresectable BTC published since 2000 [14-17]. Collectively, these findings indicate that the radiation field for BTC is not yet standardized due to the lack of a large randomized control trial and that additional studies investigating the optimal radiation field should be conducted.

The study presented here showed that chemotherapy is frequently administered in combination with RT (47% of all patients). Chemotherapy was most often administered during RT, followed by after RT. Several trials have examined the efficacy of adjuvant chemoradiation after surgery [18] or of chemoradiation for unresectable cases [19]. The National Comprehensive Cancer Network (NCCN) reported that most CCRT for BTC involved the use of 5-FU, and that CCRT with gemcitabine is not recommended due to the limited experience with and potential toxicity of this treatment. However, the use of CCRT combined with gemcitabine-containing regimens increased in Japan during the period covered by the current survey, which suggests that additional studies should be undertaken to establish the optimal sequencing of RT and chemotherapy with drugs such as gemcitabine. For chemotherapy for advanced BTC, the recent randomized control phase III ABC-02 study showed that a combination of gemcitabine and cisplatin improved overall and progression-free survival by 30% over gemcitabine alone [20]. Based on these results, the combination of gemcitabine and cisplatin can now be considered to be the standard of care as first-line chemotherapy for patients with advanced or metastatic BTC. In Japan, however, oral anticancer drugs such as TS-1 or UFT also tend to be used as adjuvant chemotherapy after RT, and only two patients in the current study were treated with a combination of gemcitabine and cisplatin after RT.

Conclusions

Patients with BTC should continue to be enrolled in prospective studies of RT with radiosensitizing agents or of RT with dose escalation methods using techniques such as IMRT. Further surveys and comparisons with results from other countries are needed for development and optimization of RT for patients with BTC in Japan.

Consent

Written informed consent was obtained from the patient for publication of this report and any accompanying images.

Abbreviations

RT: Radiotherapy; BTC: Biliary tract cancer; EBRT: External beam radiotherapy; JROSG: The Japanese radiation oncology study group; CT: Computed tomography; ILBT: Intraluminal brachytherapy; IORT: Intraoperative radiotherapy; EQD_2: The biologically equivalent dose in 2-Gy fractions; IMRT: Intensity-modulated radiotherapy; CCRT: Concurrent chemoradiotherapy; NCCN: National comprehensive cancer network.

Competing interests

The authors made no disclosures and not receive specific funding.

Authors' contributions

KO coordinated the entire study. Patient data acquisition was done by FI, HO, HO, NU, TM, NK, TT, HA, TK, TU, YI, KK, MT, YM, HY, MT, KN, and YN. Data analysis was done by FI, KO, and YY. The manuscript was prepared by FI. Corrections and/or improvements were suggested by KO and YY. Revisions were done by HO, HO, NU, TM, NK, TT, HA, TK, TU, YI, KK, MT, YM, HY, MT, KN, and YN. All authors read and approved the final manuscript.

Author details

[1]Department of Radiation Oncology, Osaka University Graduate School of Medicine, 2-2 (D-10) Yamadaoka, Suita, Osaka 565-0871, Japan. [2]Department of Radiology, Iwate Medical University, 19-1 Uchimaru, Morioka, Iwate 020-8505, Japan. [3]Department of Radiology, University of Yamanashi, 1110, Shimogato Chuo, Yamanashi 409-3898, Japan. [4]Department of Radiation Oncology, Shimane University, 1060 Nishikawatsu-cho, Matsue-shi, Shimane 690-8504, Japan. [5]Present affiliation: Department of Radiation Oncology, Tottori Prefectural Central Hospital, 730 Etsu, Tottori-shi, Tottori 680-0901, Japan. [6]Department of Radiology, Nihon University School of Medicine, 30-1, Ohyaguchi-Kamimachi, Itabashi-ku, Tokyo 173-8610, Japan. [7]Department of Radiology, Tokyo Medical University, 6-1-1, Shinjuku, Shinjuju-ku, Tokyo 160-8402, Japan. [8]Department of Radiation Oncology, Nara Medical University School of Medicine, 840 Shijo-cho, Kashihara, Nara 634-8521, Japan. [9]Division of Radiation Oncology, Shizuoka Cancer Center, 1007 Shimonagakubo, Nagaizumi Town, Shizuoka 411-8777, Japan. [10]Department of Radiology, Hamamatsu University School of Medicine, 1-20-1 Handayama, Higashi-ku, Hamamatsu city, Shizuoka 431-3192, Japan. [11]Department of Radiology, Chiba University Graduate School of Medicine, 1-8-1 Inohana, Chiba 260-8677, Japan. [12]Department of Radiation Oncology, National Cancer Center Hospital, 5-1-1 Tsukiji, Chuo-ku, Tokyo 104-0045, Japan. [13]Department of Radiation Oncology, Tokyo Metropolitan Komagome Hospital, 18-22, Honkomagome 3chome, Bunkyo-ku, Tokyo 113-8677, Japan. [14]Department of Radiology, Kyorin University School of Medicine, 6-20-2 Shinkawa, Mitaka-shi, Tokyo 181-8611, Japan. [15]Department of Radiology, Nagoya City University Graduate School of Medical Sciences, Kawasumi, Mizuho-cho, Mizuho-ku Nagoya, Aichi 467-8601, Japan. [16]Department of Radiology, Kyoto Prefectural University of Medicine, Kajii-cho, Kawaramachi-Hirokoji, Kamigyo-ku, Kyoto 602-8566, Japan. [17]Department of Radiology, Okayama University, 2-5-1 Shikata-cho, Kita-ku, Okayama-shi, Okayama 700-8558, Japan. [18]Department of Radiation Oncology, Yamagata University, 2-2-2 Iida-Nishi, Yamagata-shi, Yamagata 990-9585, Japan. [19]Department of Radiation Oncology, Kinki University Faculty of Medicine, 377-2, Ohno-Higashi, Osaka-Sayama, Osaka 589-8511, Japan.

Received: 21 December 2012 Accepted: 23 March 2013
Published: 1 April 2013

References

1. Park SW, Park YS, Chung JB, Kang JK, Kim KS, Choi JS, Lee WJ, Kim BR, Song SY: **Patterns and relevant factors of tumor recurrence for extrahepatic bile duct carcinoma after radical resection.** *Hepatogastroentelogy* 2004, **51**:1612–1618.
2. Matsuda T, Marugame T, Kamo K, Katanoda K, Ajiki W, Sobue T, Japan Cancer Surveillance Research Group: **Cancer incidence and incidence rates in Japan in 2006: based on data from 15 population-based cancer registries in the monitoring of cancer incidence in Japan (MCIJ) project.** *Jpn J Clin Oncol* 2012, **42**:139–147.
3. Bonet Beltràn M, Allal AS, Gich I, Solé JM, Carrió I: **Is adjuvant radiotherapy needed after curative resection of extrahepatic biliary tract cancers? A systematic review with a meta-analysis of observational studies.** *Cancer Treat Rev* 2012, **38**:111–119.
4. Shinohara ET, Mitra N, Guo M, Metz JM: **Radiotherapy is associated with improved survival in adjuvant and palliative treatment of extrahepatic cholangiocarcinomas.** *Int J Radiat Oncol Biol Phys* 2009, **74**:1191–1198.
5. Nishimura Y, Koike R, Ogawa K, Sasamoto R, Murakami Y, Itoh Y, Negoro Y, Itasaka S, Sakayauchi T, Tamamoto T: **Clinical practice and outcome of radiotherapy for esophageal cancer between 1999 and 2003: the Japanese radiation oncology study group (JROSG) survey.** *Int J Clin Oncol* 2012, **17**:48–54.
6. Ogawa K, Ito Y, Karasawa K, Ogawa Y, Onishi H, Kazumoto T, Shibuya K, Shibuya H, Okuno Y, Nishino S, Ogo E, Uchida N, Karasawa K, Nemoto K, Nishimura Y, JROSG Working Subgroup of Gastrointestinal Cancers: **Patterns of radiotherapy practice for pancreatic cancer in Japan: results of the Japanese radiation oncology study group (JROSG) survey.** *Int J Radiat Oncol Biol Phys* 2010, **77**:743–750.
7. Shibuya H, Tsujii H: **The structural characteristics of radiation oncology in Japan in 2003.** *Int J Radiat Oncol Biol Phys* 2005, **62**:1472–1476.
8. Teshima T, Numasaki H, Shibuya H, Nishio M, Ikeda H, Ito H, Sekiguchi K, Kamikonya N, Koizumi M, Tago M, Nagata Y, Masaki H, Nishimura T, Yamada S, Japanese Society of Therapeutic Radiology and Oncology Database Committee: **Japanese structure of radiation oncology in 2005 based on institutional stratification of patterns of care study.** *Int J Radiat Oncol Biol Phys* 2008, **72**:144–152.
9. Alden ME, Mohiuddin M: **The impact of radiation dose in combined external beam and intraluminal Ir-192 brachytherapy for bile duct cancer.** *Int J Radiat Oncol Biol Phys* 1994, **28**:945–951.
10. Lu JJ, Bains YS, Abdel-Wahab M, Brandon AH, Wolfson AH, Raub WA, Wilkinson CM, Markoe AM: **High-dose-rate remote afterloading intracavitary brachytherapy for the treatment of extrahepatic biliary duct carcinoma.** *Cancer J* 2002, **8**:74–78.
11. Milano MT, Chmura SJ, Garofalo MC, Rash C, Roeske JC, Connell PP, Kwon OH, Jani AB, Heimann R: **Intensity-modulated radiotherapy in treatment of pancreatic and bile duct malignancies: toxicity and clinical outcome.** *Int J Radiat Oncol Biol Phys* 2004, **59**:445–453.
12. Takamura A, Saito H, Kamada T, Hiramatsu K, Takeuchi S, Hasegawa M, Miyamoto N: **Intraluminal low-dose-rate 192Ir brachytherapy combined with external beam radiotherapy and biliary stenting for unresectable extrahepatic bile duct carcinoma.** *Int J Radiat Oncol Biol Phys* 2003, **57**:1357–1365.
13. Jarnagin WR, Ruo L, Little SA, Klimstra D, D'Angelica M, DeMatteo RP, Wagman R, Blumgart LH, Fong Y: **Patterns of initial disease recurrence after resection of gallbladder carcinoma and hilar cholangiocarcinoma: implications for adjuvant therapeutic strategies.** *Cancer* 2003, **98**:1689–1700.
14. Crane CH, Macdonald KO, Vauthey JN, Yehuda P, Brown T, Curley S, Wong A, Delclos M, Charnsangavej C, Janjan NA: **Limitations of conventional doses of chemoradiation for unresectable biliary cancer.** *Int J Radiat Oncol Biol Phys* 2002, **53**:969–974.
15. Brunner TB, Schwab D, Meyer T, Sauer R: **Chemoradiation may prolong survival of patients with non-bulky unresectable extrahepatic biliary carcinoma. A retrospective analysis.** *Strahlenther Onkol* 2004, **180**:751–757.
16. Shin HS, Seong J, Kim WC, Lee HS, Moon SR, Lee IJ, Lee KK, Park KR, Suh CO, Kim GE: **Combination of external beam irradiation and high-dose-rate intraluminal brachytherapy for inoperable carcinoma of the extrahepatic bile ducts.** *Int J Radiat Oncol Biol Phys* 2003, **57**:105–112.
17. Chen YX, Zeng ZC, Tang ZY, Fan J, Zhou J, Jiang W, Zeng MS, Tan YS: **Determining the role of external beam radiotherapy in unresectable intrahepatic cholangiocarcinoma: a retrospective analysis of 84 patients.** *BMC Cancer* 2010, **10**:492.
18. Nelson JW, Ghafoori AP, Willett CG, Tyler DS, Pappas TN, Clary BM, Hurwitz HI, Bendell JC, Morse MA, Clough RW, Czito BG: **Concurrent chemoradiotherapy in resected extrahepatic cholangiocarcinoma.** *Int J Radiat Oncol Biol Phys* 2009, **73**:148–153.
19. Czito BG, Anscher MS, Willett CG: **Radiation therapy in the treatment of cholangiocarcinoma.** *Oncology (Williston Park)* 2006, **20**:873–884.
20. Valle J, Wasan H, Palmer DH, Cunningham D, Anthoney A, Maraveyas A, Madhusudan S, Iveson T, Hughes S, Pereira SP, Roughton M, Bridgewater J, ABC-02 Trial Investigators: **Cisplatin plus gemcitabine versus gemcitabine for biliary tract cancer.** *N Engl J Med* 2010, **362**:1273–1281.

doi:10.1186/1748-717X-8-76
Cite this article as: Isohashi *et al.*: Patterns of radiotherapy practice for biliary tract cancer in Japan: results of the Japanese radiation oncology study group (JROSG) survey. *Radiation Oncology* 2013 **8**:76.

子宮頸癌の画像誘導小線源治療

戸板孝文／粕谷吾朗／有賀拓郎／平安名常一／垣花泰政／村山貞之

琉球大学大学院医学研究科 放射線診断治療学講座

はじめに

子宮頸癌に対し放射線治療は手術と並ぶ根治的治療法である。III期以上の進行例ではもちろんのこと、I、II期の手術可能の早期例においても、米国のガイドライン[1]のみならず本邦での治療ガイドライン[2]で根治的放射線治療は手術と並列する治療オプションの位置づけである。子宮頸癌の根治的放射線治療は、外部照射（全骨盤照射）と腔内照射の組み合わせからなる。他癌と同様に、子宮頸癌の放射線治療も2次元（2D）から3次元（3D）、さらに4次元（4D）へと進化しつつある。外部照射では臨床標的体積（clinical target volume：CTV）ベースの3D計画が普及し[3,4]、強度変調放射線治療（intensity modulated radiotherapy：IMRT）の臨床適用も進みつつある[5]。腔内照射では長らく2方向撮影されたX線画像をベースにした2D計画が行われてきたが、近年ようやくCT/MRIを用いた3D計画治療、画像誘導小線源治療（image-guided brachytherapy：IGBT）が注目されてきた[6]。

2D計画の限界

A点処方を基本としたマンチェスター法は、子宮頸癌腔内照射のスタンダードとして長らく治療の均てん化に貢献してきた。A点線量に基づく標準スケジュールが早くから確立し[7]、良好な治療成績をあげてきた[8]。直腸の晩期合併症の発生率／重症度が2D計画で規定した基準点（ICRU38）[9]での線量と関連することが報告されてきた[10]。しかし、A点線量と局所制御の線量効果関係を明確にできず[11]、膀胱合併症についてICRU38基準点での線量との相関を示せなかった[12]。特定点での線量評価を基本とし、腫瘍形状やリスク臓器全体の座標を考慮できない2D計画の限界は明らかであった。

IGBTの歴史

2D計画の限界を克服するため、CTなど3D画像を用いた腔内照射の試みが1980年代初めよりすでに開始されていた[13]。わが国でも1987年には中野らがMRIを用いた先駆的研究を報告している[14]。ウイーン大学のPotterらは1996年よりCTによるDVHベースの計画を開始した[15]。1998年よりMRIを用いた臨床応用が開始され、2000年よりGroupe Europeen de Curietherapie of the European Society for Therapeutic Radiology and Oncology（GEC-ESTRO）に3D計画を推進するWGが組織された。その後2004年にAmerican Brachytherapy Society（ABS）より[16]、2005年にGEC-ESTROより[17]ガイドラインが出版された。2005年7月にシカゴでワークショップが開催され、その後IGBTの標準化がGEC-ESTRO主導で進められることが合意された。

表1にIGBTの臨床的なメリットをまとめる。2D計画の弱点を克服し、より安全で効果的な治療を行うことが期待できる。

表1　子宮頸癌IGBTのメリット

- アプリケータと腫瘍・臓器との位置関係が把握できる
  - タンデム：子宮内腔への留置確認、穿孔の有無確認
  - オボイド：頸部、腟円蓋部との位置関係
- リスク臓器の正確な線量評価が可能（DVH）
  - 特にS状結腸、小腸の線量評価が可能（⇔2Dでは不可能）
- 腫瘍（GTV, CTV）の正確な線量評価が可能（DVH）
  - 腫瘍に対するdose conformityの改善
  - 小腫瘍例に対するdose de-escalation
  - 大腫瘍例に対するdose escalation

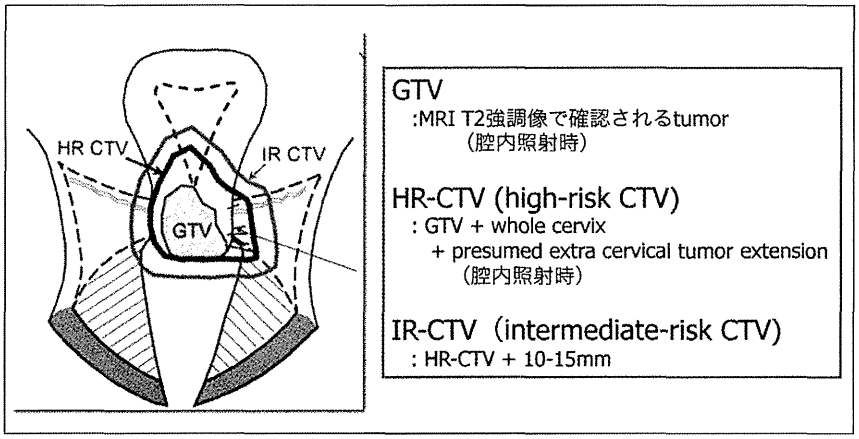

図1　子宮頸癌IGBTにおけるターゲットボリュームの定義[17]

IGBTにおける治療計画パラメータ

1）Contouring

外部照射と同様に、IGBTにおいても、ターゲットとリスク臓器の適切なcontouringは最重要の作業プロセスである。contouringのばらつきは、IGBTの線量投与に不確実性を与える最も大きな要因と考えられている[18]。

ターゲットに関しては、GEC-ESTROの定義が現在広く用いられている（**図1**）[17]。しかし、MRIをベースに作成されているため、CTを用いた計画での運用は難しい。ViswanathanらはCTを使用する場合のHR-CTVの定義を提言した[19]。彼女らは、MRIと比較してHR-CTVのD90が低めに算出されることを明らかにし、CTにて設定したHR-CTVがMRIよりも過大になることを示唆した[19]。CTの組織分解能はMRIに劣るため、腫瘍はもちろんのこと周囲の血管や炎症等と子宮頸部との分離も困難なことは少なくない（**図2**）。

リスク臓器（organ at risk：OAR）に関しても、GEC-ESTROの方法[20]を用いることが一般的である。Viswanathanらの検討では、HR-CTVの評価とは異なり、OARに関してCTはMRIと有意差がなかったことが示されている[19]。従来の2D計画では、通常OARとして直腸と膀胱のみが評価されてきた。しかし実際にCT等の3D画像にて評価すると、S状結腸や小腸も高線量が投与さ

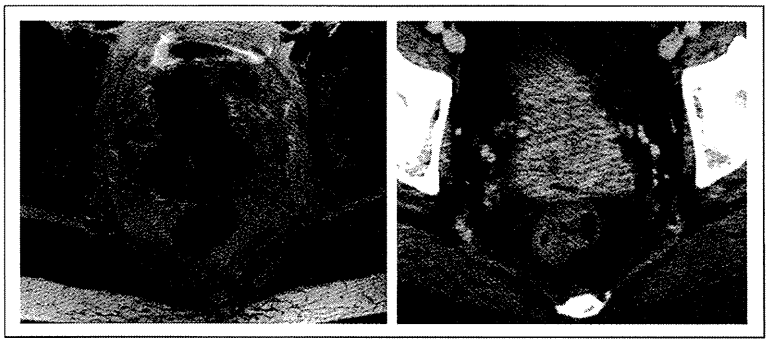

図2　同一症例におけるMRI（T2WI）とCT

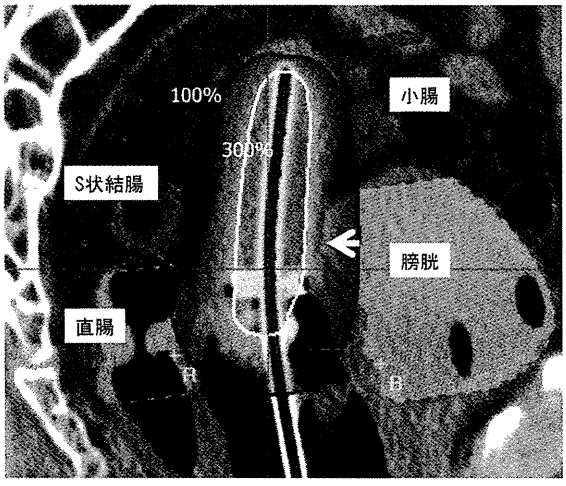

図3　R：ICRU38直腸線量評価点、B：ICRU38膀胱線量評価点
膀胱においてICRU基準点線量は許容値内であるが、矢印部で高線量が投与されている。また、S状結腸、小腸においても100%以上の線量が投与される部位があることがわかる。

れうるリスク臓器であることがわかる（**図3**）。したがって、これらの臓器もcontouringを行い評価することが推奨されている。

2）DVHパラメータ

GEC-ESTROのガイドラインではGTV、HR-CTV、IR-CTVのD100，D90を記録することを推奨している（**表2**）[20]。HR-CTVのD90が局所制御に相関したとの報告もある[21]。しかし、HR-CTVのD90に処方することに関するコンセンサスはなく、現時点ではA点で処方を行い、OARのDVHパラメータ等を確認しながら線量分布を調整し、結果としてのGTV、CTVのDVHパラメータを記録することが現実的であり推奨される。後述するように日本ではCTでの計画がほとんどであり、CTでのHR-CTVのcontouringが非常に難しいことを考えると、HR-CTVのD90処方はさらに慎重であるべきである。一方、OARに関しては、それぞれD0.1cc，D2ccを算出することが推奨されており（**表2**）[20]、晩期合併症の発生率との相関が示唆されている[22]。

3D計画の問題点と課題

表1にまとめたように、IGBTの臨床的なメリ

表2　子宮頸癌IGBTで記録されるべきパラメータ(Embrace protocol)

- A点線量(左、右、平均)
- D100: GTV, HR-CTV, IR-CTV
- D90: GTV, HR-CTV, IR-CTV
- D50: HR-CTV
- V100: HR-CTV
- D0.1cc, D2cc: bladder, rectum, sigmoid
- ICRU38評価点線量: rectum, bladder

表3　子宮頸癌IGBT実施状況

国	調査年	対象	回答率	計画用画像		
				単純X線	CT	MRI
米国(ABS)	2007	ABSメンバー	55%	*43%	*67%	*1%
カナダ	2009	放射線腫瘍医#	62%	50%	45%	5%
英国	2008	46施設	100%	73%	22%	4%
	2011	45施設	96%	26%	53%	21%
日本	2012	171施設	84%	79%	14%	1%

ABS: American Brachytherapy Society、 *US member、 #婦人科腫瘍を扱う

ットは明らかである。しかし普及と適切な適用に向けての課題は少なくない。**表3**に各国でのIGBT実施率を示す[23~26]。各国と比較し、日本ではまだまだ実施率は低い状況である。本邦を含めてIGBTの普及を阻む原因として、従来の2D計画と比較して時間と手間を要する治療であることが挙げられる。前述のアンケート調査でも、放射線治療部門でのマンパワー不足を理由にする回答が多くみられた。さらにCT/MRIへのアクセス、専用のアプリケータの普及や計画装置のスペックも大きな問題である。英国では2008年の調査で26%の実施率であったが、Royal College of Radiologists(RCR)を中心とした積極的な啓蒙活動により推進され、2011年の調査では71%と実施率が急速に増加したことが報告されている。臨床データの集積とともに、学会レベルでの推進、教育活動、さらにインフラの整備のために診療報酬の改善も重要と考えられる。

さらに、CTを用いたIGBTの標準化は重要な課題である。GEC-ESTROで推奨するMRIベースのIGBTは理想的であるが、日本で実施できる施設は非常に限られており、普及にはCTベースのIGBTを前提に考えるべきである。ウィーン大学が中心となり、MRIベースのIGBTの国際多施設臨床研究:EMBRACEが進行中である[27]。これまで26施設が参加し900例が登録されている(2013年6月)。今後CTベースのIGBTの標準化に向けたワーキンググループが国内にも組織され、活動が進められることが期待される。

参考文献

1) http://www.nccn.org/professionals/physician_gls/f_guidelines.asp
2) CQ08, CQ09 子宮頸癌治療ガイドライン2011, 金原出版, 61-72

3) Small W Jr et al: Consensus guidelines for delineation of clinical target volume for intensity-modulated pelvic radiotherapy in postoperative treatment of endometrial and cervical cancer. Int J Radiat Oncol Biol Phys 71(2): 428-34, 2008

4) Toita T et al: A consensus-based guideline defining the clinical target volume for pelvic lymph nodes in external beam radiotherapy for uterine cervical cancer. Jpn J Clin Oncol 40(5): 456-63, 2010

5) Hasselle MD et al: Clinical outcomes of intensity-modulated pelvic radiation therapy for carcinoma of the cervix. Int J Radiat Oncol Biol Phys 80(5): 1436-1445, 2011

6) Pötter R et al: Clinical outcome of protocol based image (MRI) guided adaptive brachytherapy combined with 3D conformal radiotherapy with or without chemotherapy in patients with locally advanced cervical cancer. Radiother Oncol 100(1): 116-123, 2011

7) 荒居龍雄ほか: 子宮頸癌の放射線治療基準. 癌の臨床 30: 496-500, 1984

8) Nakano T et al: Long-term results of high-dose rate intracavitary brachytherapy for squamous cell carcinoma of the uterine cervix. Cancer 103(1): 92-101, 2005

9) ICRU, International Commission on Radiation Units and Measurement "Dose and volume specification for reporting intracavitary therapy in gynecology". ICRU Report 38 1985; Bethesda, MD, USA.

10) Toita T et al: Combination external beam radiotherapy and high-dose-rate intracavitary brachytherapy for uterine cervical cancer: analysis of dose and fractionation schedule. Int J Radiat Oncol Biol Phys 1;56(5): 1344-1353, 2003

11) Petereit DG et al: Literature analysis of high dose rate brachytherapy fractionation schedules in the treatment of cervical cancer: is there an optimal fractionation schedule?. Int J Radiat Oncol Biol Phys 43(2): 359-366, 1999

12) Potter R: et al: Survey of the use of the ICRU 38 in recording and reporting cervical cancer brachytherapy. Radiother Oncol 58(1): 11-17, 2001

13) Coltart RS et al: A CT based dosimetry system for intracavitary therapy in carcinoma of the cervix. Radiother Oncol 10(4): 295-305, 1987

14) 中野隆史ほか: 子宮頸癌放射線治療におけるMRIの臨床評価. 日医放会誌 47: 1181-1188, 1987

15) Fellner C et al: Comparison of radiography- and computed tomography-based treatment planning in cervix cancer in brachytherapy with specific attention to some quality assurance aspects. Radiother Oncol 58(1): 53-62, 2001

16) Nag S et al: Proposed guidelines for image-based intracavitary brachytherapy for cervical carcinoma: report from Image-Guided Brachytherapy Working Group. Int J Radiat Oncol Biol Phys 60(4): 1160-1172, 2004

17) Haie-Meder C et al: Recommendations from Gynaecological (GYN) GEC-ESTRO Working Group (I): concepts and terms in 3D image based 3D treatment planning in cervix cancer brachytherapy with emphasis on MRI assessment of GTV and CTV. Radiother Oncol 74(3): 235-245, 2005

18) Tanderup K et al: Uncertainties in image guided adaptive cervix cancer brachytherapy: Impact on planning and prescription. Radiother Oncol 107(1): 1-5, 2013

19) Viswanathan AN et al: Computed tomography versus magnetic resonance imaging-based contouring in cervical cancer brachytherapy: results of a prospective trial and preliminary guidelines for standardized contours. Int J Radiat Oncol Biol Phys 68(2): 491-498, 2007

20) Pötter R et al: Recommendations from gynaecological (GYN) GEC ESTRO working group (II): concepts and terms in 3D image-based treatment planning in cervix cancer brachytherapy-3D dose volume parameters and aspects of 3D image-based anatomy, radiation physics, radiobiology. Radiother Oncol 78(1): 67-77, 2006

21) Dimopoulos JC et al: Dose-effect relationship for local control of cervical cancer by magnetic resonance image-guided brachytherapy. Radiother Oncol 93(2): 311-315, 2009

22) Georg P et al: Dose-volume histogram parameters and late side effects in magnetic resonance image-guided adaptive cervical cancer brachytherapy. Int J Radiat Oncol Biol Phys 79(2): 356-362, 2011

23) Viswanathan AN et al: Three-dimensional imaging in gynecologic brachytherapy: a survey of the American Brachytherapy Society. Int J Radiat Oncol Biol Phys 76(1): 104-109, 2010

24) Pavamani S et al: Image-guided brachytherapy for cervical cancer: a Canadian Brachytherapy Group survey. Brachytherapy 10(5): 345-351, 2011

25) Tan LT: Implementation of image-guided brachytherapy for cervix cancer in the UK: progress update. Clin Oncol (R Coll Radiol) 23(10): 681-684, 2011

26) Toita T, ohno T et al: Image-guided brachytherapy for cervical cancer: a questionnaire-based survey in Japan. 2nd ESTRO FORUM 2013.

27) www.embracestudy.dk

Journal of Radiation Research, 2013, 54, 569–577
doi: 10.1093/jrr/rrs123 Advance Access Publication 18 December 2012

Computer-aided beam arrangement based on similar cases in radiation treatment-planning databases for stereotactic lung radiation therapy

Taiki MAGOME[1,2], Hidetaka ARIMURA[3,*], Yoshiyuki SHIOYAMA[4], Asumi MIZOGUCHI[1], Chiaki TOKUNAGA[1], Katsumasa NAKAMURA[5], Hiroshi HONDA[5], Masafumi OHKI[3], Fukai TOYOFUKU[3] and Hideki HIRATA[3]

[1]Department of Health Sciences, Graduate School of Medical Sciences, Kyushu University, 3-1-1 Maidashi, Higashi-ku, Fukuoka 812-8582, Japan
[2]Japan Society for the Promotion of Science, 5-3-1 Kojimachi, Chiyoda-ku, Tokyo 102-0083, Japan
[3]Department of Health Sciences, Faculty of Medical Sciences, Kyushu University, 3-1-1 Maidashi, Higashi-ku, Fukuoka 812-8582, Japan
[4]Department of Heavy Particle Therapy and Radiation Oncology, Graduate School of Medical Sciences, Kyushu University, 3-1-1 Maidashi, Higashi-ku, Fukuoka 812-8582, Japan
[5]Department of Clinical Radiology, Graduate School of Medical Sciences, Kyushu University, 3-1-1 Maidashi, Higashi-ku, Fukuoka 812-8582, Japan
*Corresponding author: Division of Quantum Radiation Science, Department of Health Sciences, Faculty of Medical Sciences, Kyushu University 3-1-1, Maidashi, Higashi-ku, Fukuoka 812-8582, Japan. Tel and Fax: +81-92-642-6719; Email: arimurah@med.kyushu-u.ac.jp

(Received 11 August 2012; revised 21 November 2012; accepted 22 November 2012)

The purpose of this study was to develop a computer-aided method for determination of beam arrangements based on similar cases in a radiotherapy treatment-planning database for stereotactic lung radiation therapy. Similar-case-based beam arrangements were automatically determined based on the following two steps. First, the five most similar cases were searched, based on geometrical features related to the location, size and shape of the planning target volume, lung and spinal cord. Second, five beam arrangements of an objective case were automatically determined by registering five similar cases with the objective case, with respect to lung regions, by means of a linear registration technique. For evaluation of the beam arrangements five treatment plans were manually created by applying the beam arrangements determined in the second step to the objective case. The most usable beam arrangement was selected by sorting the five treatment plans based on eight plan evaluation indices, including the D95, mean lung dose and spinal cord maximum dose. We applied the proposed method to 10 test cases, by using an RTP database of 81 cases with lung cancer, and compared the eight plan evaluation indices between the original treatment plan and the corresponding most usable similar-case-based treatment plan. As a result, the proposed method may provide usable beam arrangements, which have no statistically significant differences from the original beam arrangements ($P > 0.05$) in terms of the eight plan evaluation indices. Therefore, the proposed method could be employed as an educational tool for less experienced treatment planners.

Keywords: radiotherapy treatment planning; similar planning cases; computer-assisted method; beam arrangements; stereotactic lung radiotherapy

INTRODUCTION

Stereotactic body radiotherapy (SBRT) has been actively performed for early stage lung cancers in recent decades [1]. The survival rate for SBRT has been encouraging, and potentially comparable to that for surgery [2]. The key to successful implementation of SBRT is appropriate beam arrangement, which generally consists of a large number of coplanar and non-coplanar beams [3]. However, the determination of beam arrangements in SBRT is a substantial

and demanding task for inexperienced treatment planners, as well as experienced treatment planners, and affects the critical dose distribution with steep dose gradients. Treatment planning skills are developed by repeated planning in clinical practice, often under the guidance of experienced planners or appropriate textbooks. In this way, treatment planners should memorize many planning patterns and construct an evolving 'database' in their memory, which can then be searched for past cases similar to the case under consideration. However, although a number of automated methods for determination of beam arrangements have been developed [4, 5], there are currently no such methods for determining beam arrangements based on similar past cases. On the other hand, in the field of diagnostic radiology, the presentation of similar cases as a diagnostic aid has been suggested for diagnosis of chest images [6], lung computed tomography (CT) images [7, 8], and mammography images [8–11]. These studies have indicated the feasibility of the usage of similar cases as a diagnostic aid. However, to the best of our knowledge, there are no studies on the feasibility of determination of beam arrangements using similar planning cases in the radiation therapy field. The purpose of this study was to develop a computer-aided method for determination of beam arrangements based on similar planning cases in a radiotherapy treatment-planning (RTP) database for stereotactic lung radiotherapy. The beam arrangement includes not only beam directions but also accelerating voltages, collimator angles, beam weights etc.

MATERIALS AND METHODS

Figure 1 shows the overall scheme of the proposed method, which consists of two main steps. First, similar cases to an objective case were searched, based on geometrical features related to structures such as the location, size, and shape of the planning target volume (PTV), lung and spinal cord. Second, beam arrangements of the objective case were automatically determined by registering similar cases with the objective case, in terms of lung structure regions using a linear registration technique, i.e. an affine transformation [12]. Finally, the similar-case-based beam arrangements were evaluated by plan evaluation indices. Details of the proposed method are described in this section.

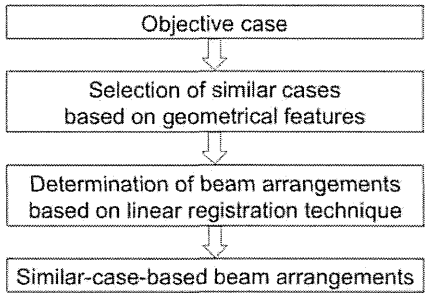

Fig. 1. Overall scheme for the determination of similar-case-based beam arrangements.

Clinical cases

This study was performed under a protocol approved by the institutional review board of the University Hospital. We selected 96 patients with lung cancer (right lung: 52 cases, left lung: 44 cases) who were treated with SBRT from November 2003 to April 2010. The patients (60 males and 36 females) had a median age of 76 years (range, 42–92 years), and their mean effective diameter of PTV was 4.0 ± 0.7 cm. Treatment planning was performed by experienced radiation oncologists on a commercially available RTP system using a pencil beam convolution algorithm (Eclipse version 6.5 and 8.1; Varian Medical Systems Inc., Palo Alto, USA). Contours of the gross tumor volumes of lung cancers were manually outlined on planning CT images acquired on a 4-slice CT scanner (Mx 8000; Philips, Amsterdam, The Netherlands) with 16-bit gray levels, a slice thickness of 2.0 mm (95 cases) or 5.0 mm (1 case), and a pixel size of 0.78 mm (29 cases), 0.86 mm (1 case), 0.88 mm (10 cases) or 0.98 mm (56 cases). The internal target volume (ITV) was created individually according to the internal respiratory motion, which was measured with an X-ray simulator (Ximatron; Varian Medical Systems Inc., Palo Alto, USA). The setup margins between the ITV and PTV were 5 mm in all directions. Seven to eight beams, including beams in the coplanar and non-coplanar directions, were arranged, depending on each patient. All patients received a dose of 48 Gy, prescribed at the isocenter in 4 fractions, with accelerating voltages of 4, 6 or 10 MV on linear accelerators (Clinac 21EX; Varian Medical Systems Inc., Palo Alto, USA).

All cases were randomly separated into three datasets, i.e. a dataset comprising the RTP database, a dataset of 5 training cases (right lung: 3 cases, left lung: 2 cases), and a dataset of 10 test cases (right lung: 3 cases, left lung: 7 cases). The RTP database thus included 81 cases (right lung: 46 cases, left lung: 35 cases). The 5 training and 10 test cases were used to determine the parameters for selection of similar cases and for the evaluation of our method, respectively.

Selection of similar planning cases using geometrical features

Beam arrangements are generally determined by considering the geometrical features in an objective case including the tumor, organs at risk (OAR) (such as spinal cord), and normal tissue structures. The geometrical features relevant in making an SBRT treatment plan for lung cancer include the PTV location, the PTV shape, the PTV size, the lung dimension, and the geometrical relationship between the PTV and the spinal cord. Therefore, it was considered reasonable to define similar cases with respect to these geometrical features.

In the first step the RTP database was searched for the 5 cases most similar to the objective case by considering the weighted Euclidean distance of geometrical feature vectors between the objective case and each case in the RTP database. The weighted Euclidean distance was thus considered a similarity measure. The weights of geometrical features were needed in order to consider the importance of the geometrical features from the treatment planning point of view. When applying the proposed method to their own databases, each institute should determine the appropriate weights of the geometrical features based on their own philosophy or policy of treatment planning. The weighted Euclidian distance d_{image} was calculated by the following equation:

$$d_{image} = \sqrt{\sum_{i=1}^{G} w_i(\alpha_i - \beta_i)^2}, \qquad (1)$$

where G is the number of geometrical features, w_i is the weight of the i-th geometrical feature, α_i is the i-th geometrical feature for the objective case, and β_i is the i-th geometrical feature for each case in the RTP database. Note that each geometrical feature was divided by standard deviation of all cases in the RTP database for normalizing the range of each feature value. In this study, we defined 10 geometrical features, i.e. the PTV centroid in the left-right (LR), anterior-posterior (AP), and superior-inferior (SI) directions, the effective diameter of the PTV, the sphericity of the PTV, the lung dimension in the LR, AP, and SI directions, the distance between the PTV and spinal cord in the isocenter plane, and the angle from the spinal cord to the PTV in the isocenter plane. The weights for geometrical features were empirically set as follows based on the institution's policy of treatment planning by using the 5 training cases with a trial and error procedure so that cases more similar to the objective case could be selected in terms of appearance relevant to the features: the PTV centroid = 0.3, effective diameter of the PTV = 0.1, sphericity of the PTV = 0.1, lung dimension = 0.3, distance between the PTV and spinal cord = 1.0, and angle from spinal cord to the PTV = 1.0. In our program, the weights for geometrical features were normalized when the similarity measure was calculated. However, we believe that it would be more logical for users to set the weights from 0 to 1.0, than to set the sum of the weights equal to 1.0. The PTV centroid was determined by registering the lung structure image of each case in the RTP database with that of a reference case based on the following linear registration technique, i.e. affine transformation [12]:

$$\begin{pmatrix} p' \\ q' \\ r' \\ 1 \end{pmatrix} = \begin{pmatrix} u_{11} & u_{12} & u_{13} & u_{14} \\ u_{21} & u_{22} & u_{23} & u_{24} \\ u_{31} & u_{32} & u_{33} & u_{34} \\ 0 & 0 & 0 & 1 \end{pmatrix} \begin{pmatrix} p \\ q \\ r \\ 1 \end{pmatrix}, \qquad (2)$$

where the transformation parameters $u_{11} \ldots u_{34}$ were determined based on feature points. We used a special case of an affine transformation including only the translation and scaling due to two feature points, where the affine transformation parameters u_{12}, u_{13}, u_{21}, u_{23}, u_{31}, and u_{32} were resulted to zero. The remaining transformation parameters were determined by analytically solving simultaneous equations based on two feature points. The vertices of a circumscribed parallelepiped of a lung, including left and right lung regions, were automatically obtained as feature points for calculation of parameters of the affine transformation matrix as follows. First, the minimum and maximum x, y and z coordinates, x_{min}, x_{max}, y_{min}, y_{max}, z_{min} and z_{max}, were obtained in the original coordinate system of the planning CT image from the lung segmented by a treatment planner, and then six planes of $x = x_{min}$, $x = x_{max}$, $y = y_{min}$, $y = y_{max}$, $z = z_{min}$ and $z = z_{max}$ were determined as those of the circumscribed parallelepiped. Finally, two vertices of the circumscribed parallelepiped of the lung region (x_{min}, y_{min}, z_{min}) and (x_{max}, y_{max}, z_{max}) were used as feature points for determination of parameters in the affine transformation matrix. In this study, the circumscribed parallelepiped was chosen to reduce the calculation time for finding the feature points of the lung. As the registration, the PTV centroid of each case, located at (p, q, r), would move to the position (p', q', r') in the coordinate system of a reference case by Equation 2. The effective diameter was defined as the diameter of a sphere with the same volume as the PTV. The sphericity was defined as the roundness of the PTV without a directional dependence, and given by the ratio of the number of logical AND voxels between the PTV and its equivalent sphere with the same centroid and volume as the PTV to the number of PTV voxels. In fact, we employed the sphericity in this study as a similarity measure for finding similar cases in terms of tumor roundness. In future, when determining beam directions, we should take into account the direction of tumor regions as one of the shape features for retrieving similar cases.

Lung dimensions were defined as three side-lengths of the circumscribed parallelepiped of the lung regions in the LR, AP and SI directions. The distance between the PTV and the spinal cord was measured between the centroid of the PTV and that of the spinal cord in the isocenter plane. The angle from the spinal cord to the PTV was defined in the 2D coordinate system with the origin at the centroid of the spinal cord in the isocenter plane, and ranged from $-\pi$ (clockwise) to π (counterclockwise) for a baseline of the posterior-anterior direction. Although only the PTV centroid was determined in a fixed reference coordinate system by registering the lung regions of each case in the RTP database with those of a reference case; other features were calculated on each original coordinate system. This was to consider the relative similarity of the tumor in lung regions, as well as the absolute similarity such as lung dimensions and spinal cord position.

Determination of beam arrangements based on the linear registration technique

In the second step, five beam arrangements (each of which had seven or eight beam directions) for an objective case were automatically determined by registration of five similar cases with the objective case in terms of lung regions using a linear registration technique, i.e. affine transformation [12]. The beam arrangement of the similar case was modified to fit the objective case with respect to lung regions. Please note that linear registration maps straight lines to straight lines, and thus the beam directions, which can be considered as lines with the origin at the isocenter, are uniquely and automatically determined by the registration of the lung regions. First, the affine transformation matrix of Equation 2, registering the lung regions of each similar case with those of the objective case, was calculated based on two feature points, which were automatically selected for the registration in vertices of the circumscribed parallelepiped of the lung regions. Second, a beam angle, i.e. beam direction vector, based on a gantry angle θ and couch angle ϕ, was transformed from a spherical polar coordinate system to a Cartesian coordinate system as unit direction vector (a, b, c) as follows:

$$\begin{pmatrix} a \\ b \\ c \end{pmatrix} = \begin{pmatrix} \sin\theta\cos\phi \\ -\cos\theta \\ \sin\theta\sin\phi \end{pmatrix}. \tag{3}$$

Third, each beam direction vector of the similar case in the Cartesian coordinate system was modified by using the same affine transformation matrix of Equation 2 as a registration in terms of lung regions. Finally, the resulting direction vector (a', b', c') in the Cartesian coordinate system was converted into the spherical polar coordinate system as the gantry angle θ' and the couch angle ϕ' as follows:

$$\theta' = \tan^{-1}\left(\frac{\sqrt{a'^2 + c'^2}}{-b'}\right), \tag{4}$$

$$\phi' = \tan^{-1}\left(\frac{c'}{a'}\right). \tag{5}$$

Evaluation of beam arrangements using plan evaluation indices

Five treatment plans were manually made, based on the beam arrangements with other planning parameters (accelerating voltages, collimator angles, beam weight, etc.) derived from treatment plans of similar cases in a radiation treatment-planning system. Users of our system can manually select among the treatment plans provided by the proposed method with their own policies, depending on patient performances. In this study, however, the most usable treatment plan of the objective case was automatically selected by sorting the five plans based on an RTP evaluation measure with eight plan evaluation indices (which was the Euclidean distance in a feature space between each treatment plan and an ideal treatment plan) for evaluation of beam arrangements determined by the similar cases. The beam arrangement of the similar case except beam directions was used for that of an objective case as they are or after a minor modification of the accelerating voltage if needed.

In this study, the ideal treatment plan was assumed to produce perfectly uniform irradiation, with a prescription dose in the PTV and no irradiation in the surrounding OAR and normal tissues. The usefulness of each treatment plan was estimated by the following Euclidean distance d_{plan} of the plan evaluation vector between the ideal treatment plan and each treatment plan determined by a similar case, and designated the 'RTP evaluation measure':

$$d_{plan} = \sqrt{\sum_{j=1}^{J} (X_j - Y_j)^2}, \tag{6}$$

where J is the number of plan evaluation indices, X_j is the j-th plan evaluation index for the ideal treatment plan, and Y_j is the j-th plan evaluation index for the treatment plan based on the five most similar cases. Each plan evaluation index was normalized by the standard deviation in the same manner as the geometrical features based on the RTP database including 81 cases. The eight evaluation indices consisted of the D95, the homogeneity index (HI), the conformity index (CI) for the PTV, V5, V10, V20, mean dose for the lung, and maximum dose for the spinal cord, and their values for the ideal treatment plan were set to 48 Gy (prescription dose), 1.0, 1.0, 0%, 0%, 0%, 0 Gy, and 0 Gy, respectively. We evaluated similar-case-based beam arrangements suggested by the proposed method using Equation 6 based on the Euclidean distance of eight plan evaluation indices. Although we could have applied weights to plan evaluation indices based on planners' preferences, in this study we decided to give a constant weight to each plan evaluation index.

The plan evaluation indices for the PTV calculated in this study were the D95, HI and CI, which are described below:

D95: minimum dose in the PTV that encompasses at least 95% of the PTV.

HI: dose uniformity in the PTV, defined as the ratio of the maximum dose to the minimum dose in the PTV [13].

CI: degree of conformity, defined as the ratio of the treated volume to the PTV. The treated volume is defined as the tissue volume that is intended to receive at least the selected dose, and is specified by the radiation oncologist as being appropriate to achieve the purpose of the treatment [14]. In this study, the treated volume was defined as the volume receiving the minimum target dose.

The plan evaluation indices for normal tissues, i.e. the lung and spinal cord, were calculated as described below. For the lung volume, which was defined as the total lung volume minus the PTV, a V5, V10, V20, and mean dose were calculated. The Vk was defined as the percentage of the total lung minus the PTV receiving $\geq k$ Gy. The maximum dose for the spinal cord was also calculated.

Assessment of the proposed method

The proposed method was assessed with an RTP database including 81 cases with lung cancer (right lung: 46 cases, left lung: 35 cases) by comparing the original beam arrangements of 10 test cases (right lung: 3 cases, left lung: 7 cases), which were randomly chosen from all 96 cases, with the corresponding most usable beam arrangements determined from similar cases. The test cases were not included in the RTP database, and were not used for determination of the weights of geometrical features. The similar cases were selected from cases that have ipsilateral lung cancers with the test case. The same beam weights and wedges of the similar cases were used for the objective cases. The irradiation fields were adjusted to the tumor using a multi-leaf collimator with an additional margin of 5 mm around the PTV.

RESULTS

Figure 2 shows an objective case with a tumor on the lung wall (Fig. 2a) and the first to fifth most similar cases (Fig. 2b–f) to the objective case. The similar cases geometrically resemble the objective case (Fig. 2a), especially in terms of the geometrical relationship between the tumor and the spinal cord. Moreover, the tumors are located on the lung wall, because the relative location of the PTV in the reference lung regions was used for the selection of similar cases. Figure 3 shows a treatment plan obtained by the original beam arrangement (Fig. 3a), and five treatment plans determined by similar-case-based beam arrangements (Fig. 3b–f), which were sorted in descending order, based on the RTP evaluation measure. The treatment plans of Fig. 3b, c, d, e and f were derived from similar cases, as shown in Fig. 2b, c, e, f and d, respectively. In this case, the beam arrangements consisted of 7–8 beams, including 3–4 coplanar beams and 3–4 non-coplanar beams. The objective case (Fig. 3a) received an oblique lateral beam, which passed close to the spinal cord in order to increase the conformity of the PTV. On the other hand, the most usable similar-case-based beam arrangement (Fig. 3b) had no lateral beams for avoiding the exposure of the spinal cord, but the second to fifth usable cases (Fig. 3c–f) had lateral beams due to prioritizing the PTV conformity over the sparing of the spinal cord. Figure 4 shows the dose volume histograms (DVHs) of the original treatment plan (Fig. 3a) and the first to third most usable treatment plans determined by the RTP evaluation measure (Fig. 3b–d). The first most usable treatment plan resulted in better PTV conformity, as well as better sparing of the lung tissue and spinal cord, compared with the original treatment plan. DVH curves of the second and third most usable treatment plans were not always better than those of the original treatment plan.

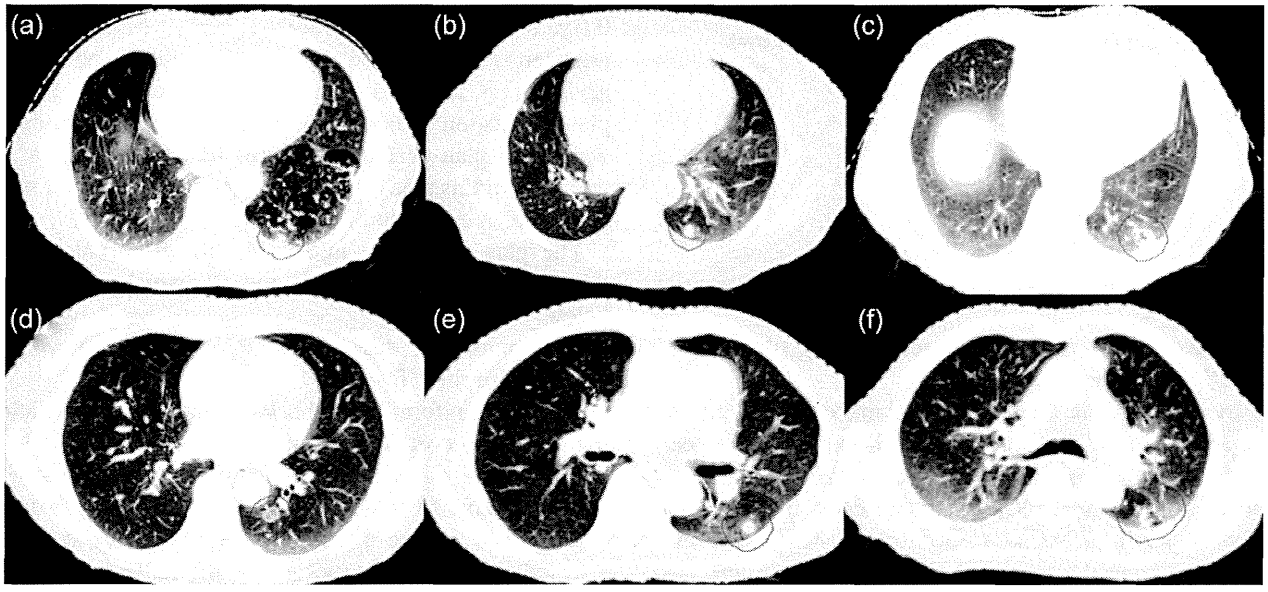

Fig. 2. An objective case (**a**) with a tumor on the lung wall, and the first to fifth most similar cases (**b–f**), which geometrically resemble the objective case, especially in terms of the geometrical relationship between the tumor and the spinal cord. Red lines indicate the planning target volumes.

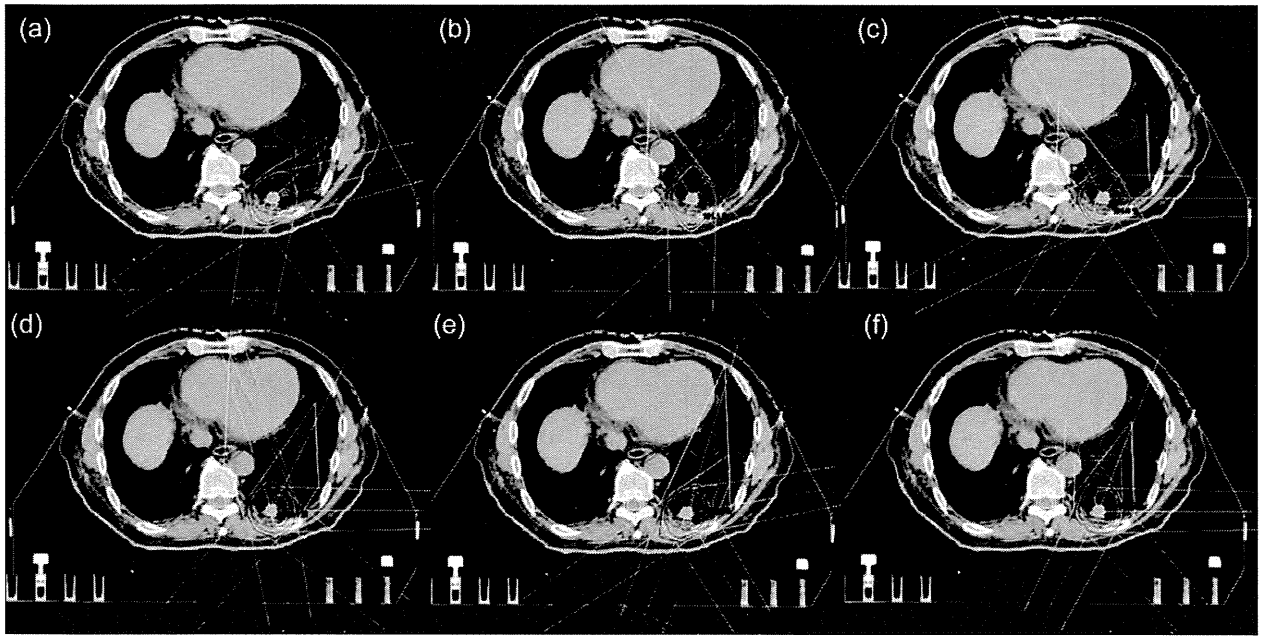

Fig. 3. A treatment plan obtained by the original beam arrangement (**a**), and 5 treatment plans determined by similar-case-based beam arrangements (**b–f**), which were sorted in descending order based on the RTP evaluation measure. The treatment plans of (b), (c), (d), (e), and (f) were derived from the similar cases as shown in Fig. **2** (b), (c), (e), (f), and (d), respectively.

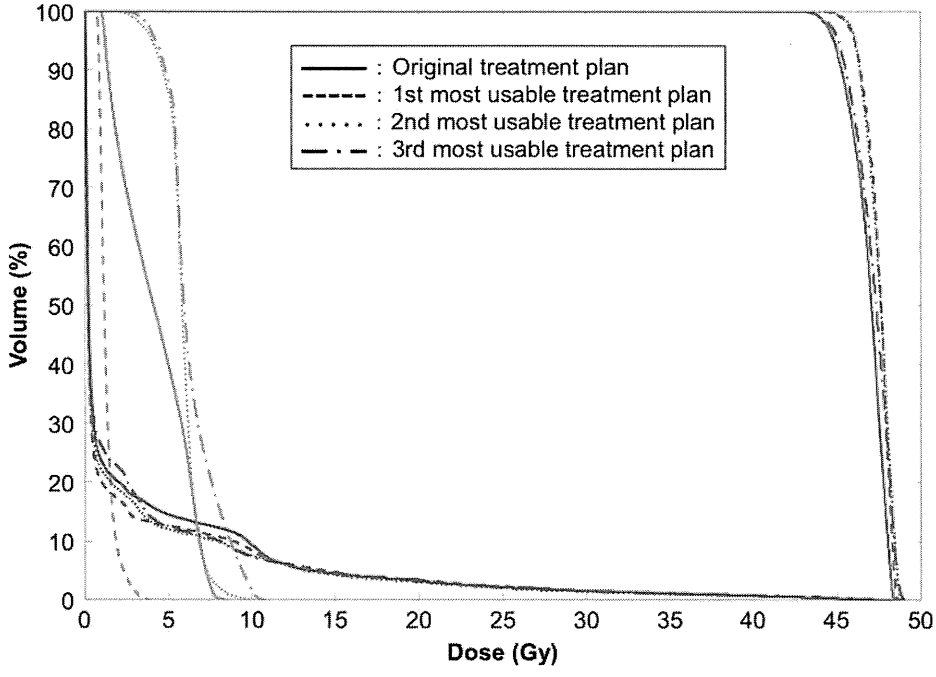

Fig. 4. Dose volume histogram comparison between treatment plans based on the original beam arrangement (solid lines) and similar-case-based beam arrangement (dotted lines): planning target volume (red), lung (blue) and spinal cord (green).

Table 1 shows the mean ± standard deviation (SD) of the plan evaluation indices in 10 test cases obtained from the dose distributions produced by original beam arrangements and similar-case-based beam arrangements (of the most usable treatment plans, as determined by the RTP evaluation measure). There were no statistically significant differences

Table 1. Mean ± standard deviation of the plan evaluation indices in 10 test cases obtained from the dose distributions produced by original and similar-case-based beam arrangements

	Original beam arrangement	Similar-case-based beam arrangement
PTV		
D95 (Gy)	45.5 ± 0.47	45.8 ± 0.62
Homogeneity index	1.13 ± 0.03	1.13 ± 0.04
Conformity index	1.70 ± 0.15	1.74 ± 0.18
Lung		
V5 (%)	16.0 ± 6.30	14.4 ± 4.98
V10 (%)	9.96 ± 4.52	9.10 ± 3.08
V20 (%)	3.98 ± 1.46	4.06 ± 1.29
Mean dose (Gy)	3.03 ± 1.11	2.90 ± 0.93
Spinal cord		
Maximum dose (Gy)	6.13 ± 3.62	8.21 ± 7.23

There were no statistically significant differences between the original beam arrangements and similar-case-based beam arrangements ($P > 0.05$).

between the original beam arrangements and the similar-case-based beam arrangements ($P > 0.05$) in terms of the eight plan evaluation indices.

DISCUSSION

In general, the RTP database in each hospital has been generated, intentionally or unintentionally, by experienced planners after many trials, and incorporates a lot of their knowledge and skills. The aim of this study was to make use of these records of knowledge and skills. Therefore, we proposed a computer-aided method for determination of beam arrangements using similar past cases in an RTP database. The proposed method could provide several usable beam arrangements based on similar cases in the RTP database. In Fig. 3b–f, the 5 usable similar-case-based beam arrangements are presented. Although the plan evaluation indices were calculated for the evaluation of the treatment plans based on the similar-case-based beam arrangements, the indices may not cover all aspects of the dose distribution. Therefore, users can manually select one of the treatment plans within their own policies, instead of the most usable treatment plan being selected automatically using plan evaluation indices.

Although SBRT has been widely used for the treatment of lung cancer in clinical practice, treatment-planning skills are required for determination of the appropriate beam direction for SBRT, which consists of a number of beams with coplanar and non-coplanar directions. Our proposed method can automatically determine beam arrangements based on the treatment plans of similar cases. If inexperienced, or less trained, treatment planners with respect to SBRT employ the proposed system using an RTP database of experienced planners, the quality of radiotherapy could be normalized among planners with different levels of experience. The proposed system could thus be used as an educational tool for treatment planners with limited SBRT experience.

Figure 5 shows the histograms of d_{image} in three test cases with right lung cancers (Fig. 5a) and left lung cancers (Fig. 5b). The means ± SDs of d_{image} for right and left lung cancer cases were 1.03 ± 0.37 and 1.28 ± 0.39, respectively. There are the small number of more similar (smaller d_{image}) cases to the test cases with the RTP database used in this study. In addition, the d_{image} was distributed with almost the same SD in the right and left lung cancer cases. Figure 6 shows the distribution of the d_{plan} for 50 treatment plans in 10 test cases. The mean ± SD of the d_{plan} was 6.54 ± 1.95. The distribution of the d_{plan} ranged widely from 3.0 to 12.0. Figure 7 shows the relationship between the d_{image} and the d_{plan} for 50 similar-case-based treatment plans in 10 test cases. The total correlation coefficient between the d_{image} and the d_{plan} was –0.52, but there seems to be little correlation between them in each test case. The mean ± SD of the correlation coefficient in each test case was 0.13 ± 0.37. The reason for this would be related to the dependence of similar-case-based beam arrangements on the quality of the treatment plans in the RTP database. In each test case, the most similar case did not always suggest the most usable beam arrangement. Therefore, we should study a similar-case-based optimization method for beam arrangements, including beam weights and wedges for the objective case, in future work.

The number of similar cases to be presented to planners can be determined by the preference of treatment planners. However, if planners used a relatively larger number of similar cases than 5 cases, dissimilar cases could be selected as 'similar' cases due to limited number of cases in the RTP database. In addition, it would be time-consuming for treatment planners to determine the suitable beam arrangement from too many options in routine clinical use of the proposed method. Therefore, treatment planners could change the number of similar cases, which is a flexible parameter, to adapt to each clinical situation.

The essential parameters in the proposed method were the weights of the geometrical features in Equation 1, which were needed for considering the priority of the various geometrical features from the treatment-planning point of view. In this study, we empirically determined the weights for the geometrical features as follows, based on the institution's policy of treatment planning. We used five training cases with a trial and error procedure so that the cases most similar to the objective case could be selected

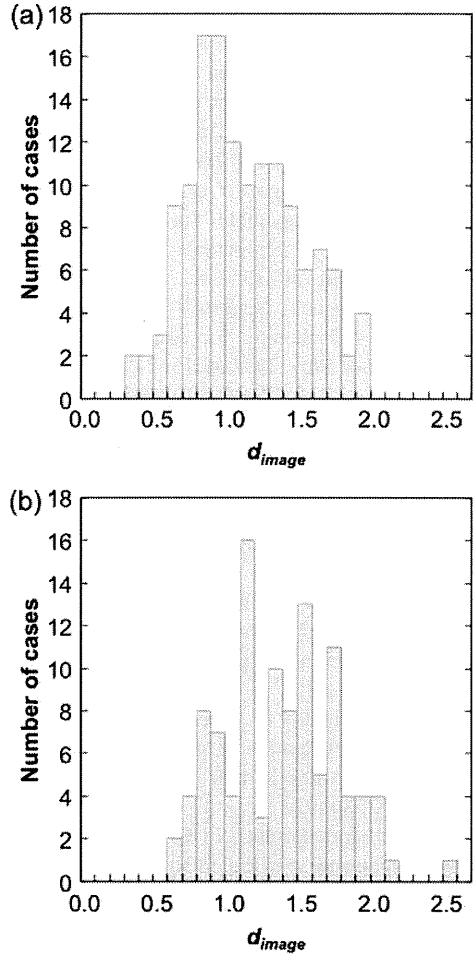

Fig. 5. Histograms of the d_{image} for selection of similar cases in three test cases (**a**) with right lung cancers and (**b**) left lung cancers.

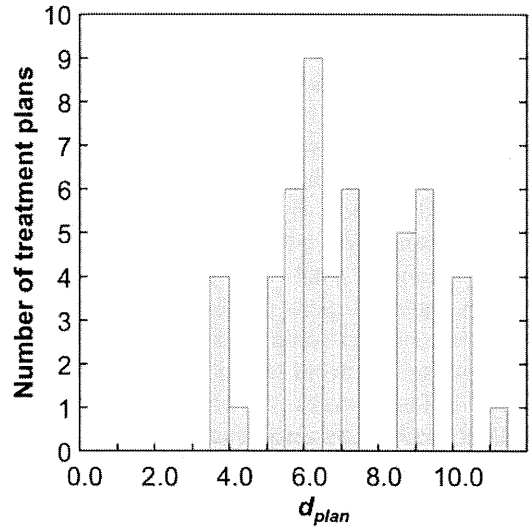

Fig. 6. Histograms of the d_{plan} for evaluation of similar case-based beam arrangements in 50 treatment plans of 10 test cases.

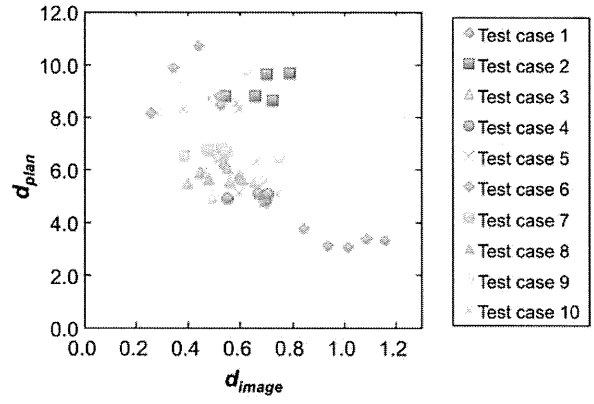

Fig. 7. Relationship between the d_{image} for selection of similar cases and d_{plan} for evaluation of similar case-based beam arrangements.

in terms of appearance relevant to the features: the PTV centroid = 0.3, the effective diameter of the PTV = 0.1, the sphericity of the PTV = 0.1, lung dimension = 0.3, the distance between the PTV and spinal cord = 1.0, and the angle from the spinal cord to the PTV = 1.0. We gave greater importance to the geometrical features related to the spinal cord in order to reduce the extra dose to the spinal cord, whereas shape features were given lower importance, because we believe that shape should play a more minor role in selection of similar cases. The weights were empirically determined using five training cases, so that the cases most similar to the objective case could be selected based on the planning viewpoints, i.e. the philosophies and policies regarding treatment planning, of a radiation oncologist (YS) and a medical physicist (HA). Therefore, when applying the proposed method to their own databases, treatment planners should first determine the appropriate weights of the geometrical features based on their own philosophies or policies regarding treatment planning. Nevertheless, it would be useful to develop the optimization method for the weights in Equation 1 so as to reduce planning time in future work, so that the planners' philosophies and policies can be incorporated into the optimization method, while retaining flexibility.

It would be very important to evaluate the results of the proposed method displayed in Table 1 from a clinical standpoint. According to our results, the proposed method may provide usable beam arrangements with little statistical difference from cases in the RTP database, as shown in Table 1. However, 56% of the plan evaluation indices were improved by the proposed method, compared with those of the original treatment plans. From the clinical point of view, the proposed method might not always suggest the

most usable treatment plans, because the quality of similar-case-based treatment plans depends on that of treatment plans in the RTP database. Therefore, the quality of the database might influence similar-case-based beam arrangements; if inappropriate treatment plans were included in the database this could be one of the limitations of the proposed method. In this study the original beam arrangements were determined by experienced radiation oncologists in our hospital, and the radiation oncologists approved all treatment plans as clinically acceptable. Even so, we need to consider some threshold values for the RTP evaluation measure to avoid selection of inappropriate treatment plans. In future works, we would like to build a more reliable RTP database by reviewing the clinical outcome of each case, and/or adding the treatment plans that were developed by the experienced radiation oncologists in regional center hospitals, and develop a method for avoiding selection of inappropriate treatment plans.

Many kinds of similarity measures have been developed for identifying similar cases in the field of diagnostic radiology [15]. We used the weighted Euclidean distance, which is one of the simple similarity measures [15], for selection of similar treatment plans, because the users of the proposed method can easily change the weights of the various geometrical features, depending on their treatment philosophies. However, other similarity measures may identify more similar treatment plans. Therefore, in future work we should investigate the efficient similarity measure for the selection of similar cases from the treatment-planning point of view. Moreover, for the assessment of the proposed method, the beam weights and wedges were set at the same values as the similar cases, but this may not be optimal for the objective case. Therefore, it will be necessary to optimize beam weights and wedges for the objective case in future work.

CONCLUSIONS

We have proposed a technique to determine computer-aided beam arrangement for stereotactic lung radiotherapy based on similar planning cases in an RTP database of experienced planners, and have investigated its feasibility. The results have shown that the proposed method provides usable beam arrangements with little statistical difference from cases in the RTP database. Therefore, our proposed method could be used as a tool for educating less-experienced treatment planners from an RTP database of more experienced planners. The quality of radiotherapy could thus be normalized among planners having different levels of experience in SBRT.

FUNDING

This work was supported by a Grant-in-Aid from the Japan Society for the Promotion of Science (JSPS) Fellows, and Scientific Research (c), 22611011.

REFERENCES

1. Nagata Y, Wulf J, Lax I *et al.* Stereotactic radiotherapy of primary lung cancer and other targets: results of consultant meeting of the International Atomic Energy Agency. *Int J Radiat Oncol Biol Phys* 2011;**79**:660–9.
2. Onishi H, Shirato H, Nagata Y *et al.* Stereotactic body radiotherapy (SBRT) for operable Stage I non-small-cell lung cancer: can SBRT be comparable to surgery? *Int J Radiat Oncol Biol Phys* 2011;**81**:1352–8.
3. Takayama K, Nagata Y, Negoro Y *et al.* Treatment planning of stereotactic radiotherapy for solitary lung tumor. *Int J Radiat Oncol Biol Phys* 2005;**61**:1565–71.
4. Meyer J, Hummel SM, Cho PS *et al.* Automatic selection of non-coplanar beam directions for three-dimensional conformal radiotherapy. *Br J Radiol* 2005;**78**:316–27.
5. de Pooter JA, Méndez Romero A, Wunderink W *et al.* Automated non-coplanar beam direction optimization improves IMRT in SBRT of liver metastasis. *Radiother Oncol* 2008; **88**:376–81.
6. Aisen AM, Broderick LS, Winer-Muram H *et al.* Automated storage and retrieval of thin-section CT images to assist diagnosis: system description and preliminary assessment. *Radiology* 2003;**228**:265–70.
7. Li Q, Li F, Shiraishi J *et al.* Investigation of new psychophysical measures for evaluation of similar images on thoracic CT for distinction between benign and malignant nodules. *Med Phys* 2003;**30**:2584–93.
8. Kumazawa S, Muramatsu C, Li Q *et al.* An investigation of radiologists' perception of lesion similarity: observations with paired breast masses on mammograms and paired lung nodules on CT images. *Acad Radiol* 2008;**15**:887–94.
9. Muramatsu C, Li Q, Suzuki K *et al.* Investigation of psychophysical measure for evaluation of similar images for mammographic masses: preliminary results. *Med Phys* 2005; **32**:2295–304.
10. Muramatsu C, Li Q, Schmidt RA *et al.* Determination of similarity measures for pairs of mass lesions on mammograms by use of BI-RADS lesion descriptors and image features. *Acad Radiol* 2009;**16**:443–9.
11. Muramatsu C, Schmidt RA, Shiraishi J *et al.* Presentation of similar images as a reference for distinction between benign and malignant masses on mammograms: analysis of initial observer study. *J Digit Imaging* 2010;**23**:592–602.
12. Burger W, Burge MJ. *Digital Image Processing: an Algorithmic Introduction Using Java,* 1st edn. New York: Springer, 2007.
13. Kadoya N, Obata Y, Kato T *et al.* Dose-volume comparison of proton radiotherapy and stereotactic body radiotherapy for non-small-cell lung cancer. *Int J Radiat Oncol Biol Phys* 2011;**79**:1225–31.
14. International Commission on Radiation Units and Measurements (ICRU). Prescribing, recording and reporting photon beam therapy. (Supplement to ICRU Report 50) *ICRU Report 62.* Bethesda: ICRU, 1999.
15. Müller H, Michoux N, Bandon D *et al.* A review of content-based image retrieval systems in medical applications—clinical benefits and future directions. *Int J Med Inform* 2004;**73**:1–23.

Technology in Cancer Research and Treatment
ISSN 1533-0346
2013 March 26. Epub ahead of print.

Can a Belly Board Reduce Respiratory-induced Prostate Motion in the Prone Position? – Assessed by Cine-magnetic Resonance Imaging

www.tcrt.org
DOI: 10.7785/tcrt.2012.500334

K. Terashima, M.D.[1]
K. Nakamura, M.D.[1]*
Y. Shioyama, M.D.[1]
T. Sasaki, M.D.[1]
S. Ohga, M.D.[1]
T. Nonoshita, M.D.[1]
T. Yoshitake, M.D.[1]
K. Atsumi, M.D.[2]
K. Asai, M.D.[1]
M. Hirakawa, M.D.[2]
S. Anai, Ph.D.[2]
H. Yoshikawa[2]
H. Honda, M.D.[1]

[1]Department of Clinical Radiology, Graduate School of Medical Sciences, Kyushu University, Fukuoka, Japan
[2]Department of Radiology, Kyushu University Hospital at Beppu, Beppu, Japan

The purpose of this study is to evaluate the real-time respiratory motion of the prostate and surrounding tissues/organs in the supine and prone positions and to investigate, using cine-MRI, whether a belly board can reduce respiratory-induced motion in the prone position. Cine-MRI scans were made of 13 volunteers in the supine and prone positions on a flat board and in two different prone positions using a belly board. Images in cine mode were recorded for 20 seconds. For each session, the points of interest (POIs) were located at the apex, base, mid-anterior surface and mid-posterior surface of the prostate; the tip of the seminal vesicle; the pubic symphysis; and the sacrum. The maximum range and standard deviation (SD) of the displacement from the mean value were calculated. The SDs for each of the four different positions were compared using a paired *t*-test. Respiratory-induced prostate motion was significantly larger in the prone position than in the supine position. However, when a belly board was used in the prone position, motion in the prostate and surrounding tissues/organs was significantly reduced. There were no significant differences between the two different positions using a belly board in any of the POIs.

Key words: Prostate cancer; Radiotherapy; Intrafraction motion; Cine-MRI; Belly board.

Introduction

Although it is well known that the prostate position varies in response to changes in bladder and rectal filling (1), respiratory-induced motion of the prostate has not traditionally been considered in prostate cancer radiotherapy. However, it has recently become clear that prostate motion occurs in accordance with the respiratory cycle (2-5). Therefore, the respiratory-induced motion of the prostate may be considered a factor in locating and reducing intrafraction motion during treatment planning.

In the published literature, variations have been shown in the results between the use of the prone and supine positions for prostate cancer radiotherapy. Several authors have demonstrated that the rectal irradiation dose was reduced in the prone position (6, 7), though it may be that the daily setup reproducibility is less accurate for the prone position, primarily due to systematic setup variations (7). In particular, it has been shown, using implanted radiopaque prostate markers and fluoroscopy, that ventilatory movement in the prostate is substantial in the prone position (2-4). A study using cine-magnetic resonance imaging (cine-MRI) also demonstrated that the amplitude of the respiratory-induced motion in the supine position is smaller than that in the prone position (5).

Abbreviations: POIs: Points of Interest; SD: Standard Deviation.

*Corresponding author:
Katsumasa Nakamura, M.D.
Phone: +81-92-642-5695
E-mail: nakam@radiol.med.kyushu-u.ac.jp

A belly board is frequently used as a positioning device when patients are irradiated in the prone position (8-10). Several studies have shown that the volume of irradiation to the small bowel during pelvic radiotherapy was reduced by using the prone position with a belly board (8, 9), even in cases in which the treatment was combined with intensity-modulated radiotherapy (10). However, it is not clear whether a belly board can reduce respiratory-induced motion in the prostate.

This study aimed to evaluate the real-time respiratory motion in the prostate and surrounding tissues/organs in the supine and prone positions, and to investigate using cine-MRI whether a belly board can reduce respiratory motion in the prone position.

Materials and Methods

Patients

Thirteen normal male volunteers were included in this study. Their median age was 66 years (range 28-67 years). Those who had a history of abdominal surgery or prostatic disease were excluded from this study. All volunteers gave their informed consent before the investigation began, after being provided with a detailed explanation of the scope and methods to be used. Each volunteer was asked not to empty his bladder for 1 h before the imaging sessions. No rectal protocol was specified before the imaging sessions. Volunteers were asked to breathe normally during the examination. This study was approved by the Institutional Review Board of Kyushu University Hospital.

MRI

Cine-MRI scans were made of each volunteer in the prone and supine positions on a flat board and then in two different prone positions using a belly board. The belly board was constructed of polyurethane foam and measured 157.5-cm long, 45.5-cm wide, and 8.3-cm thick and had a quadrangular opening in the center with longitudinal and transverse dimensions of 30.5 cm. To detect the influence of different belly board positions, the belly board was placed in two different positions. The positioning of the patient on the belly board can be described as follows: the lower edge of the opening of the belly board was placed near the anterior superior iliac spine (BB1 position), and near the pubic symphysis (BB2 position). A body coil was loosely applied. The scans were performed with a 1.5-T system (Magnetome Essenza; Siemens Medical Systems, Erlangen, Germany) using a single-slice segmented True-FISP cine sequence (repetition time/echo time of 4.25 msec/1.69 msec, 56° flip angle). To detect the respiratory motion of the prostate, real-time cine images (6-mm slice thickness) were acquired on the mid-sagittal plane every 1 second for 2 minutes. An image data acquisition matrix of 256 × 256 was used with a rectangular field of view of 250 mm, which resulted in a pixel size of 0.98 × 0.98 mm. In order to focus on evaluating the respiratory-induced motion, cine mode images of consecutive 20 seconds, in which there considered to be least peristaltic motion in the rectum and the body position was considered most stable, were chosen.

Points of Interest

For each session, the points of interest (POIs) were identified anatomically by one observer (K.T.). They were located at the apex, base, mid-anterior surface and mid-posterior surface of the prostate; the tip of the seminal vesicle; the pubic symphysis; and the sacrum (Figure 1).

The positions of the POIs were recorded on each cine-MRI image using the automatic measurement software PV Studio 2D (OA Science, Miyazaki, Japan). The maximum range and standard deviation (SD) of the displacement from the mean value were calculated based on the absolute values of measurements in the anteroposterior and craniocaudal dimensions. Finally, the SDs for the four different positions (supine, prone, BB1, BB2) were compared using a paired *t*-test. All statistical analyses were carried out using JMP Version 6 (SAS Institute, Cary, NC). $P < 0.05$ was considered statistically significant.

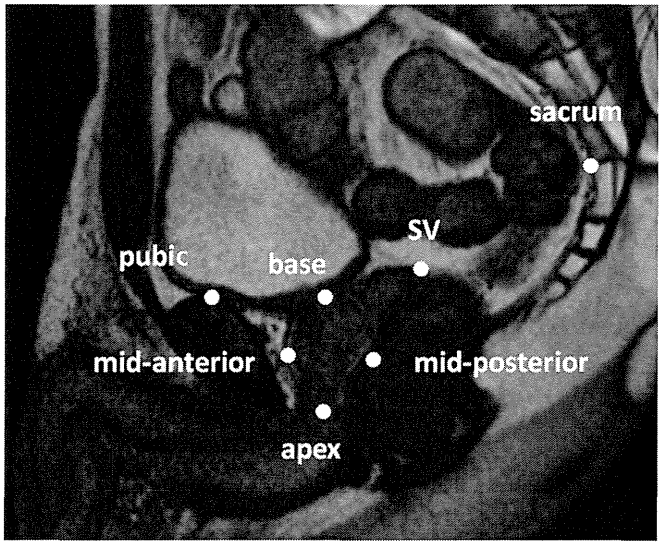

Figure 1: Location of points of interest on the mid-sagittal plane; apex, base, mid-anterior surface and mid-posterior surface, tip of the seminal vesicle (SV), pubic symphysis, and sacrum.

Results

The real-time cine-MRI sequences demonstrated that the prostate and surrounding tissues/organs moved synchronously with respiration in all 13 volunteers. Examples of subtraction images between inspiration and expiration are shown in Figure 2. The meanings of these images are that the area in which the structures were still recognized indicates more motion and the area in which the structures were almost disappeared indicates less motion.

In the prone position, respiration caused significant motion in the prostate and abdominal tissues/organs. In contrast, the prostate motion was weaker in the supine position, although motion in the abdominal tissues/organs was observed. As for the BB1 and BB2 positions, the motion of the prostate was reduced compared to that in the prone position.

The maximum ranges for each volunteer's POIs are presented in Figure 3.

There was individual variation in the motion of the prostate, including the tip of the seminal vesicle, in all positions.

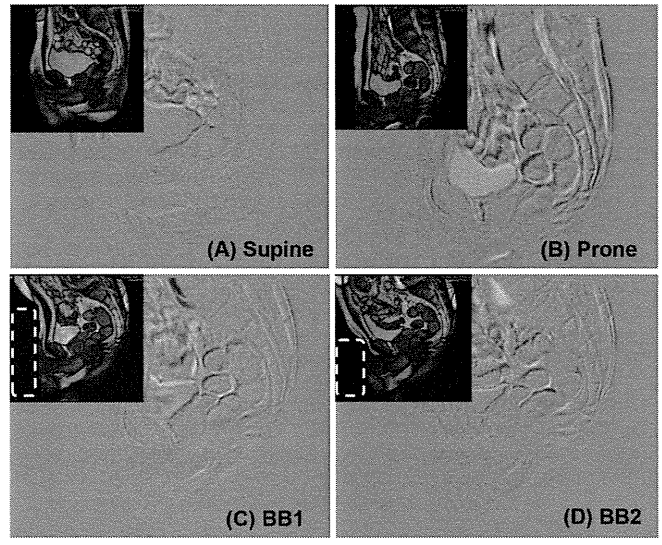

Figure 2: Examples of motion in the (**A**) Supine, (**B**) Prone, (**C**) BB1, and (**D**) BB2 positions. The original images were acquired at the ends of the inspiration and expiration phases, and the individual pixel values were subtracted. Differences in position show up as black and white areas. The dotted line indicates the position of the belly board.

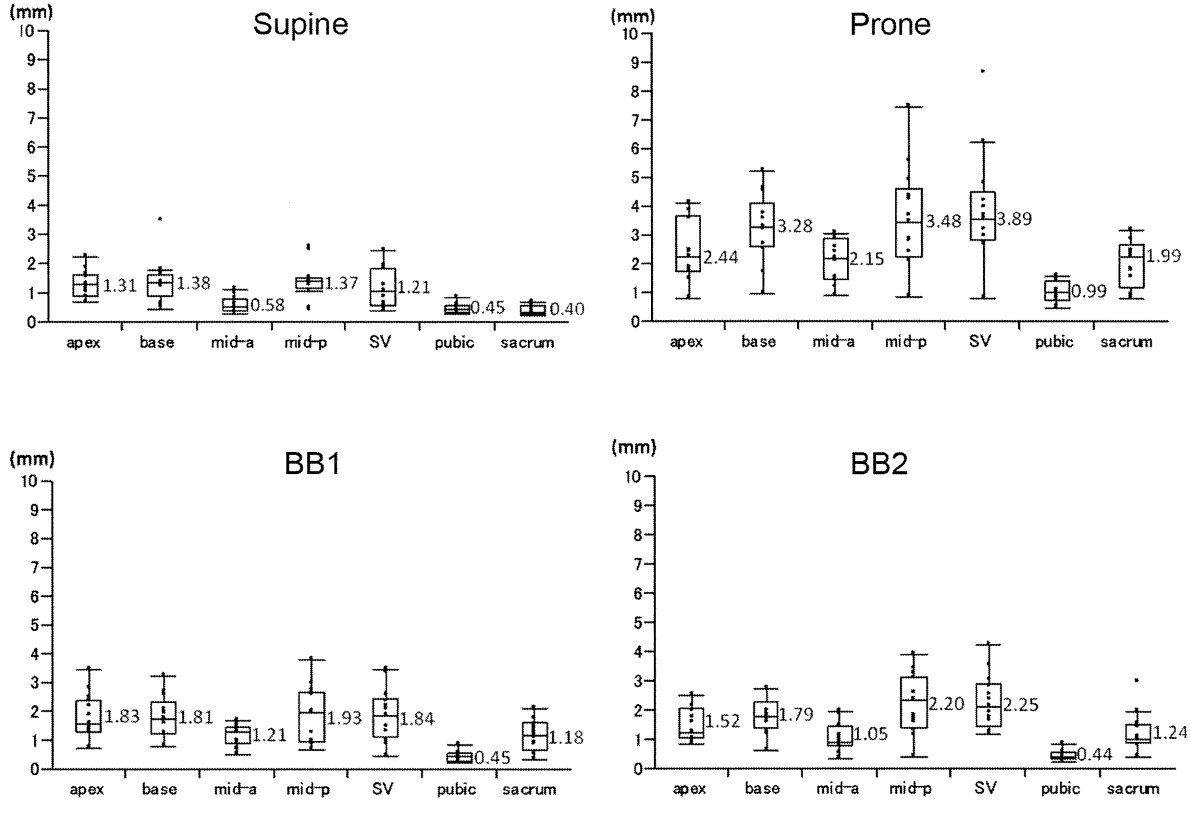

Figure 3: Box and whisker plot of the maximum range of all volunteers for each point of interest over 20 seconds. The central boxes represent values from the lower to upper quartile (25th to 75th percentiles). The middle line represents the median. The vertical line extends from the minimum to maximum values and shows the presence of outliers. The values beside the boxes indicate the means of the maximum ranges for each POIs. Abbreviations: mid-a = Mid-anterior surface; mid-p = Mid-posterior surface; SV = The tip of the seminal vesicle.

On the other hand, at the pubic symphysis, there was little motion or individual variation in any of the positions. As for the sacrum, there was little motion or individual variation in the supine position, although more individual variation was observed in the other positions.

The distribution of the SDs of the POIs is summarized in Figure 4.

Respiratory-induced prostate motion was significantly larger in the prone position than in the supine position at any POIs ($p < 0.01$). However, when a belly board was used in the prone position, compared the prone position to the BB1 or BB2 positions, the motion of the prostate and surrounding tissues/organs was suppressed significantly ($p < 0.05$) at any POIs. In the supine position, there was significantly less motion than in the BB1 and BB2 positions at the mid-anterior

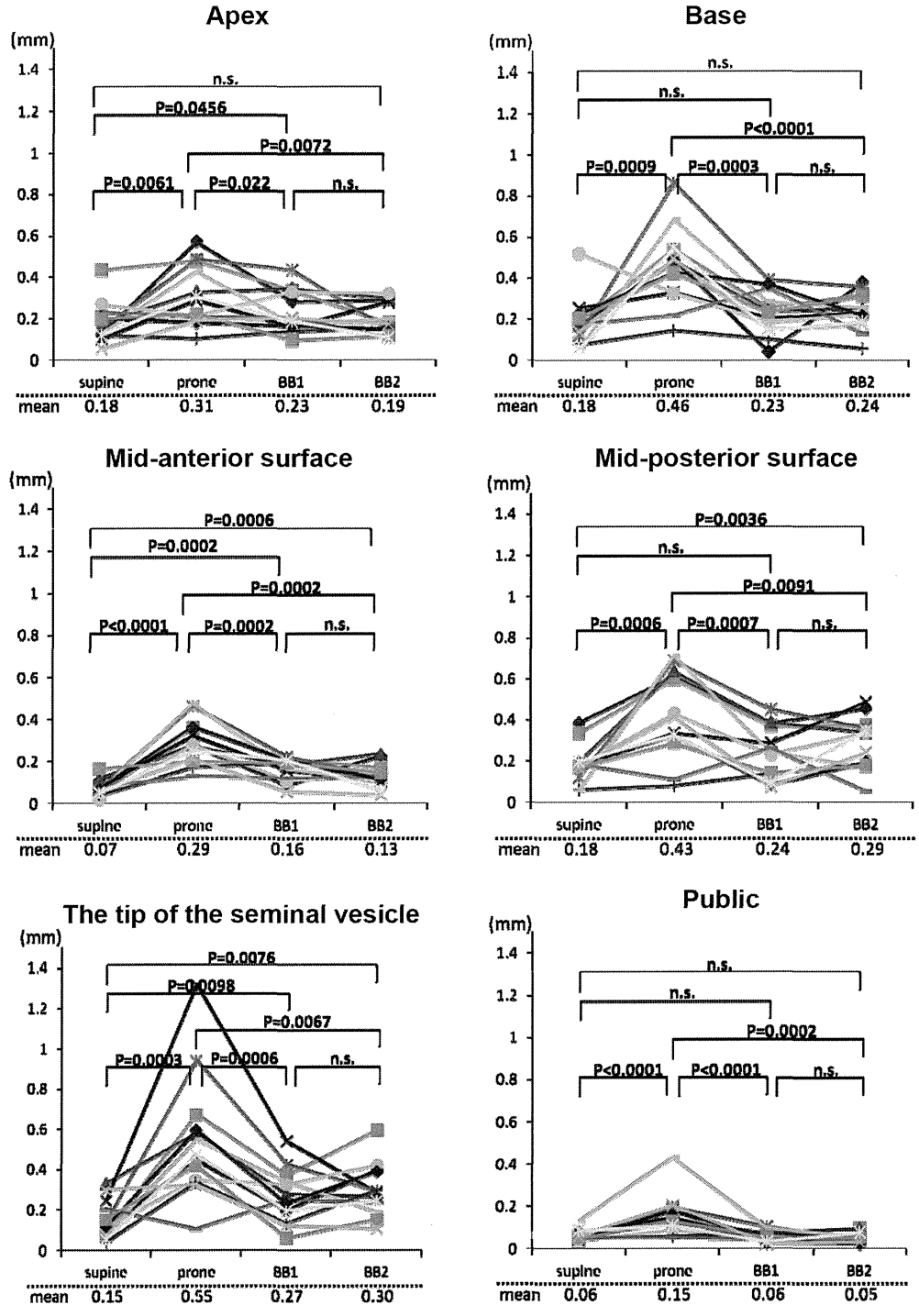

Figure 4: (*Continued*).